On the line shift and oscillator strength of Xe II lines in the spectra of HnMn stars

H. O. Di Rocco[1,2], A. Cruzado[3,4], and P. E. Marchiano[3]

[1] Intituto de Física Arroyo Seco (IFAS), Centro de Investigaciones en Física e Ingeniería del Centro de la Provincia de Buenos Aires (CIFICEN), Universidad Nacional del Centro de la Provincia de Buenos Aires (UNCPBA)-Consejo Nacional de Investigaciones Científicas y Técnicas (CONICET), Pinto 399, 7000 Tandil, Buenos Aires, Argentina
e-mail: hdirocco@exa.unicen.edu.ar
[2] Consejo Nacional de Investigaciones Científicas y Técnicas (CONICET) 1917, Argentina
[3] Facultad de Ciencias Astronómicas y Geofísicas, Univesidad Nacional de La Plata, Paseo del Bosque s/n, 1900 La Plata, Buenos Aires, Argentina
e-mail: acruzado@fcaglp.unlp.edu.ar
[4] Instituto de Astrofísica de La Plata (CONICET), Paseo del Bosque s/n, 1900 La Plata, Buenos Aires, Argentina

ABSTRACT

Aims. The ultimate goal that has motivated this work is to achieve realistic oscillator strength (gf) values to find reliable values of stellar abundances. We aim to compare the gf valúes of Xe II lines found with different theoretical and experimental methods.
Methods. We have undertaken calculations using the quasirelativistic and relativistic Hartree-Fock methods. Then we compare these results with those previously obtained from UVES spectra of HgMn stars.
Results. 1) Our theoretical gf values are more realistic than those previously obtained for most lines. When we consider only unblended, isolated, relatively noise-free lines, however, our theoretical gf values and Yuce's stellar values differ little from each other. 2) In a discussion of the origin of the previously observed discrepancy between the wavelengths of Xe II lines deducted from stellar spectra and those published by National Institute of Standards and Technology (NIST), we conclude that stellar wavelengths could be considered the standard wavelengths whenever the densities in stellar atmospheres are smaller than 1×10^{16} part. cm^{-3}.

Key words. atomic data – line: identification – stars: abundances – stars: chemically peculiar

1. Introduction

Not long ago, Yuce et al. (2011) published a work where oscillator strengths of 100 Xe II lines were inferred from UVES spectra of four HgMn stars: HR 6000, HD 71066, 46 Aql, and HD 175640. With the starting model parameters derived from photometry, the authors used, in turn, the codes ATLAS9, SYNTHE, ATLAS12, and WIDTH to obtain synthetic spectra and abundances of many elements and ions, among them Xe II. In principle, this work is the more extensive source of "experimental" oscillator strength (gf) values for Xe II, as can be verified by comparing with the National Institute of Standards and Technology (NIST) database.

In addition, Yuce et al. (2011) considered blueshifts up to 0.1 Å from the predicted wavelength of some Xe II lines (according to the established level scheme), of a priori unidentified stellar lines. Since similar shifts are characteristic of the high current discharges used in many laboratories to obtain Xe spectra, the data of Yuce et al. (2011) provide a good standard to compare laboratory measurements affected by plasma effects (see below).

With respect to the works made about the Xe II spectrum, since the early papers published in the '30s by Humphreys et al. (1931), Boyce (1936), and Humphreys (1939), several works have been completed regarding energy levels and spectrum of Xe II, transitions probabilities, line shifts, and widths. On the basis of the published material, Hansen & Persson (1987) reported

a revised and complete analysis of the data. Extensive analysis of Xe spectra were performed at the Centro de Investigaciones Ópticas (CIOP, La Plata, Argentina). Some of these works (Persson et al. 1988; Gallardo et al. 1993) are related to Xe II, and they were used as sources of data by Saloman (2004) in his critical compilation.

In particular for Xe II, several works have been published by different authors from 1986 to date. A complete database can be found at the NIST, compiled by Kramida & Fuhr (2015).

It is important to highlight that most of the Xe II lines analyzed in the article of Yuce et al. (2011) are weak, noised and/or blended, as it is viewed on the web page of Castelli (2011), where the UVES spectra of the stars are shown. In the last section, we analyze the behavior of some lines that are referred by the authors as without blend or noise in the stellar spectra of HR 6000 (see Table 2).

We are very interested in achieving realistic gf values to find reliable values of stellar abundances, since inaccuracies in the values of gf directly translate into inaccuracies in the calculation of stellar abundances. Therefore, we focus on analyzing and comparing the gf values of Xe II lines obtained with different methods, both theoretical and experimental. Since the gf values of Yuce et al. (2011) disagree, in general, with other experimental and theoretical works (Di Rocco et al. 2000, and references therein), we have undertaken new calculations using the quasirelativistic Hartree-Fock and relativistic Hartree-Fock

methods, which are mandatory approaches because of the relatively high Z of Xe.

We organize this paper as follows: in Sect. 2 we describe the technique we have used in obtaining the atomic Xe II structure and spectra; in Sect. 3 we present our work methodology and our results; and in Sect. 4 we present our conclusions.

2. Obtaining the structure and spectra of Xe II

As is well known in modern spectroscopic analysis, once a number of levels have been found by empirical spectrum analysis, the theory can be used to calculate "the best" possible wavefunctions and, from these, radiative and collisional parameters (gf values, excitation, and ionization cross sections, etc.). Of paramount importance in the theoretical calculations is the concept of configuration interaction. The "experimental" wavefunctions are expressed in terms of the Hartree-Fock orbitals, which are taken as the base functions. So, the configurations 5s5p6 and 5s2 5p4 (6s + 7s + 8s + 5d + 6d + 7d + ...), for example, can be treated together and pure designations are, many times, of little or null significance. Then, a given $|\gamma J\rangle$ level is expressed as $|\gamma J\rangle = \sum_\beta y_{\beta j}^\gamma |\beta J\rangle$ in terms of the H-F base functions $|\beta J\rangle$ (Cowan 1981). It is expected that an expansion with a manageable small set of $|\beta J\rangle$ functions can be sufficient to give reasonable gf values if the configurations are judiciously chosen (especially if the configurations have the same principal quantum number and/or the energies of the configurations are similar).

Taking into account that the empirical structure of Xe II is well known (Hansen & Persson 1987), we have proceeded to perform calculations using the set of versatile codes from Cowan (1981). These codes are based on a quasirelativistic configuration interaction approach, allowing a least-squares fitting of the levels. With these codes, we worked in three different ways: i) We consider the electrostatic Slater parameters, F^2(5p; 5p), F^2(5p; nl), G^k(5p; nl), and R^k(ij; tu), and the spin-orbit parameter, ϕ_{nl}, from the least-squares adjustment of the levels (semiempirical analysis) of Hansen & Persson (1987); we call this the Hansen-Persson least-squares (HPLS) approach. ii) We select the same configurations of Hansen & Persson (1987), but perform the purely ab initio calculations with proper scaling factors; we call this the Hansen-Persson Ab Initio (HPAI) approach. iii) We use an extended set of congurations judiciously chosen in a purely theoretical form; we call this the Ab Initio Many Congurations (AIMC) approach.

The theoretical results, obtained through the HPLS, HPAI, and AIMC approaches, have already been analyzed and compared, among themselves, and with the experimental approaches; e.g., Di Rocco et al. (2000). Reaffirming their conclusions, we find that the three approaches are all reasonably consistent and, therefore, some degree of quality can be conferred to all our calculations. Given this, we may choose any set of theoretical results to compare them with the results of Yuce et al. (2011), which is our aim. We may also take into consideration all of our theoretical results and obtain a final result as

$$gf = \tilde{gf} \pm \frac{\sqrt{\sum_i \left(\tilde{gf} - (gf)_i\right)^2}}{N}. \tag{1}$$

Furthermore, we have used the code FAC from Gu (2008). This is a fully relativistic MultiConfiguration Dirac-Hartree-Fock (MCDHF) approach, widely used in recent years. It is important to highlight that the two sets of gf values, obtained with the

FAC and Cowan codes, are very similar. Clearly, we can use the gf values of different codes and generalize the Eq. (1).

With that in mind, the aim of this article can be achieved by comparing the theoretical results obtained with either approach outlined above with those of Yuce et al. (2011). Therefore, to simplify and streamline our research, we use the results we obtained with the HPLS approach to work.

3. Calculations and results

3.1. The calculation of the oscillator strengths

Following Cowan's nomenclature (1981), the calculation of transition probabilities, A_{ij}, and related weighted oscillator strengths, gf_{ij}, are related to the calculation of line strength

$$S_{ij} = \left|\left\langle \gamma J \left\| P^{(1)} \right\| \gamma' J' \right\rangle\right|^2, \tag{2}$$

where $P^{(1)}$ is the dipole moment of the atom measured in units of $-ea_0$. When the energies are measured in Rydbergs, the relation between gf and S is given by

$$gf = \frac{E_j - E_i}{3} S. \tag{3}$$

The states $|\gamma J\rangle = \sum_i a_i \phi_i$ and $|\gamma' J'\rangle = \sum_i a'_i \phi'_i$ can be constructed basically in two ways: configuration interaction and multiconfiguration expansions. In the first case, the coefficients a_i are fixed by the theory and the ϕ_i are optimized; in the second case, both the a_i and the ϕ_i are optimized. The more useful codes using the CI approach are Cowan's (quasirelativistic) and Gu's (relativistic) codes; among others, the MCDHF approach is due to Froese Fischer (1997) and Grant (2007). We use the two CI treatments from Cowan and Gu because both of those are free and straightforward to use. In our opinion, the methodology of Cowan is convenient: we can use a least-squares fit of the levels and scale the radial factors (Slater integrals F^k, G^k and ζ_{nl}) in that process. Then, that scaling process indirectly takes several difficult aspects of the many atom theory (exchange, correlation, etc.) into account.

3.2. A brief about the line widths and shifts

When atoms and ions are immersed in plasma characterized by their electron temperature, T_e, and electron density, N_e, the energy levels are shifted with respect to the ideal situation of the "isolated" atom (Griem 1964). Furthermore, the spectral lines are broadened because the collisions with free electrons shorten the lifetime of the excited electrons in the atoms. There are diverse mechanisms of plasma broadening but, because in the laboratory experiments the spectra of Xe II are obtained using high current pinched discharges ($T_e \approx 1-2$ eV, $N_e \approx 1 \times 10^{16}-1 \times 10^{17}$ cm^{-3}), the more important mechanisms are those generically called pressure broadening (in particular, interactions with charged particles), which are treated mathematically via the impact approximation (Griem 1997; Sobelman et al. 1995).

Although we do not make explicit calculations about shifts (d) and widths (w), we recall that the calculation of both, d and w, as well as the behavior of T_e and N_e, are very complex (see Sahal-Bréchot et al. 2014, as well as Peláez et al. 2009a,b). Summing up, in the semiclassical approximation both, shifts and broadenings, are basically proportional to $N_e T_e^{-1/2}$.

Regarding d, whereas for $6p-6d$ and $6p-7s$ transitions $d \approx 0.1$ Å, for $6s-6p$ and $5d-6p$ transitions d is, in general, much lower because the initial and final levels are shifted almost the same amount. Stark parameters of some XeII lines were measured by Peláez et al. (2009a,b) for the $6p-6d$, $6p-7s$, $6s-6p$ and $5d-6p$ transitions. For the two last cases, experimental errors are, sometimes, a significant percentage of the measured Stark shifts. For comparison, it is important to establish that in the works of classical atomic spectroscopy, where the lines are measured on photographic plates, the accuracy is, typically, of the order of 0.01 Å.

3.3. Results

3.3.1. General trends

To begin with, we compare the gf values published by Yuce et al. (2011) with our theoretical gf values. From our calculations carried out, including the 5s2 5p4 6p, 5s 5p6, 5s2 5p4 6s, 5s2 5p4 7s, 5s2 5p4 8s, 5s2 5p4 5d, 5s2 5p4 6d, and 5s2 5p4 7d configurations, we have been able to identify 91 of the 98 lines for which Yuce et al. (2011) have found stellar gf values. In Table 1, third and fourth columns, the stellar gf values, obtained by Yuce et al. (2011), and the theoretical values we obtained with the Cowan Code, are shown for these 91 lines. For these 91 Xe II lines, we analyze, at first, the ratio between our theoretical gf values and the gf values inferred by Yuce et al. (2011) from UVES spectra of HgMn stars, $gf_{\mathrm{th}}/gf_{\mathrm{st}}$. From this preliminary analysis, it has been apparent that some lines are too far away from the theoretical values to be adjusted. Therefore, we eliminate seven lines for which the ratio $gf_{\mathrm{th}}/gf_{\mathrm{st}} > 6$ from any subsequent analysis. Our intention is not to do a line-by-line comparison, but rather to assess general trends and behaviors.

We believe that, perhaps, the shift between the stellar and theoretical gf values for the remaining 84 lines could be reduced by adjusting the radial integrals entering the gf calculation. We adjusted these radial integrals for each pair of atomic configurations to achieve the best possible fit for all lines arising from the pair. In Fig. 1, panels a) and b), we show two possible fits. In both panels, the logarithm of stellar gf values are shown as a function of the theoretical values. The adjustment for the 84 Xe II lines is shown in panel a). In an attempt to improve this adjustment, we eliminted nine lines and obtained the fit shown in panel b). In Table 1, fifth and sixth columns, the theoretical gf values are displayed for the 84 and 75 lines used in the first and second adjustment, respectively. Two important things have to be pointed out. First, adjusting the radial integrals does not significantly improve the correlation. In any case, the linear correlation coefficients take values between $r = 0.61$ and $r = 0.63$, as well as when nine lines are eliminated. Second, the factors that multiply the radial integrals range from 1.15 to 1.9 vary very little from one adjustment to another. Even if the correlation had improved, these factors that multiply the integrals are too large to account for the differences between the theoretical gf values to the stellar values.

In order to find some general trends in the ratio $gf_{\mathrm{th}}/gf_{\mathrm{st}}$, in Fig. 2 this ratio is shown as a function of λ. In panel a) the 84 lines are included. In panel b) seven lines have been removed to demonstrate that a clear correlation exists between the ratio $gf_{\mathrm{th}}/gf_{\mathrm{st}}$ and λ. From Fig. 2 it seems that some systematic source of error is affecting the results.

Table 1. Stellar and theoretical gf values.

λ (Å)	Conf.	$\log(gf_{\mathrm{st}})$	$\log(gf_{\mathrm{th}})$	$\log(gf_{\mathrm{th,ad1}})$	$\log(gf_{\mathrm{th,ad2}})$
3907.820	6p6d	−0.82	−0.1220	−0.6636	−0.6827
4037.260	6p6d	−1.00	−0.8190	−1.3597	−1.3788
4037.470	6p6d	−0.75	−0.0710	−0.6126	−0.6317
4057.360	6p6d	−0.80	−0.3240	−0.8658	−0.8849
4157.980	6p6d	−0.60	0.0280	−0.5122	−0.5313
4162.160	5d6p	−1.57	−0.9460	−1.0668	−1.0992
4180.007	6d6p	−0.35	0.2350	−0.3060	−0.3251
4193.100	6d6p	−0.60	0.6950		
4208.391	6d6p	−0.38	0.1520	−0.3893	−0.4084
4209.370	6d6p	−0.70	−0.1420	−0.6836	−0.7027
4213.620	6p6d	−0.22	0.3250	−0.2173	−0.2364
4215.620	6s6p	−1.05	−0.6390	−0.8524	−0.8944
4222.900	6p6d	0.64	0.1220	−0.4210	
4238.135	6p6d	−0.23	0.3240	−0.2173	−0.2364
4245.300	6p6d	−0.13	0.5110	−0.0310	−0.0501
4251.540	6p6d	−0.58	0.1150	−0.4276	−0.4467
4330.390	6p6d	0.30	0.5200	−0.0217	−0.0408
4369.100	6p6d	−0.72	−0.1500	−0.6915	−0.7106
4373.700	6p6d	−0.70	−0.1370	−0.6788	−0.6979
4393.090	6p6d	0.00	0.5330	−0.0088	−0.0279
4395.770	6p6d	0.00	0.8260		
4416.090	6p6d	−0.80	0.1330		
4448.025	6p6d	0.10	0.7160	0.1745	0.1554
4462.090	6p6d	0.33	0.8190	0.2773	0.2582
4787.770	5d6p	−0.82	−0.6350	−0.7544	−0.7868
4817.980	5d6p	−1.25	−0.9000	−1.0195	−1.0519
4823.250	6p7s	−0.65	−0.1070	−0.4832	−0.4832
4844.330	6s6p	0.61	0.5140	0.3004	
4876.500	6s6p	0.10	0.2660	0.0530	0.0110
4883.530	6s6p	−0.25	−0.0010	−0.2150	−0.2570
4884.090	6p7s	−0.80	−0.3690	−0.7450	−0.7450
4887.300	6s6p	−0.85	−0.4380	−0.6519	−0.6939
4890.085	6s6p	−1.17	−0.7690	−0.9837	−1.0257
4919.660	5d6p	−0.85	−0.5030	−0.6229	−0.6553
4921.480	6s6p	0.05	0.3020	0.0869	0.0449
4972.700	6s6p	−0.55	−0.1220	−0.3362	−0.3782
4988.725	5d6p	−0.85	−0.4820	−0.6014	−0.6338
5044.920	6s6p	−0.80	−0.2500	−0.4644	−0.5064
5080.510	6p7s	−0.22	0.1380	−0.2397	−0.2397
5122.310	6p7s	−0.37	−0.3050	−0.6818	−0.6818
5188.080	6p7s	−1.10	0.1710		
5260.420	5d6p	−0.37	−0.2750	−0.3948	−0.4272
5261.950	6s6p	0.25	0.1390	−0.0743	
5268.250	5d6p	−0.80	−1.1640	−1.2842	−1.3166
5292.220	6s6p	0.49	0.4290	0.2156	
5309.270	6s6p	−0.95	−0.5320	−0.7458	−0.7878
5313.760	6p7s	−0.09	0.2650	−0.1116	−0.1116
5339.355	6s6p	−0.10	0.0540	−0.1611	−0.2031
5368.075	5d6p	−1.05	−1.9600	−2.0785	−2.1109
5372.405	6s6p	−0.15	−0.1420	−0.3562	−0.3982
5419.155	6s6p	0.37	0.3460	0.1322	
5438.960	6s6p	−0.44	−0.1360	−0.3503	−0.3922
5450.450	5d6p	−0.97	−4.4930	−4.6134	−4.6458
5460.365	5d6p	−0.77	−0.6010	−0.7202	−0.7526
5472.600	5d6p	−0.55	−0.3540	−0.4735	−0.5059
5531.050	5d6p	−0.78	−0.6610	−0.7814	−0.8138
5616.650	5d6p	−0.70	0.4582		
5659.380	6s6p	−0.65	−0.3530	−0.5668	−0.6088

Notes. The first and second columns list the wavelength and the configurations which originate the lines. In the third column the values of $\log(gf)$ inferred by Yuce et al. (2011) are shown. In the fourth column the values of $\log(gf)$ given by the code Cowan are indicated. The values of $\log(gf)$ given by the code Cowan after adjusting Slater integrals, for two different groups of lines (see text for explanation), are exhibited in the fifth and sixth columns.
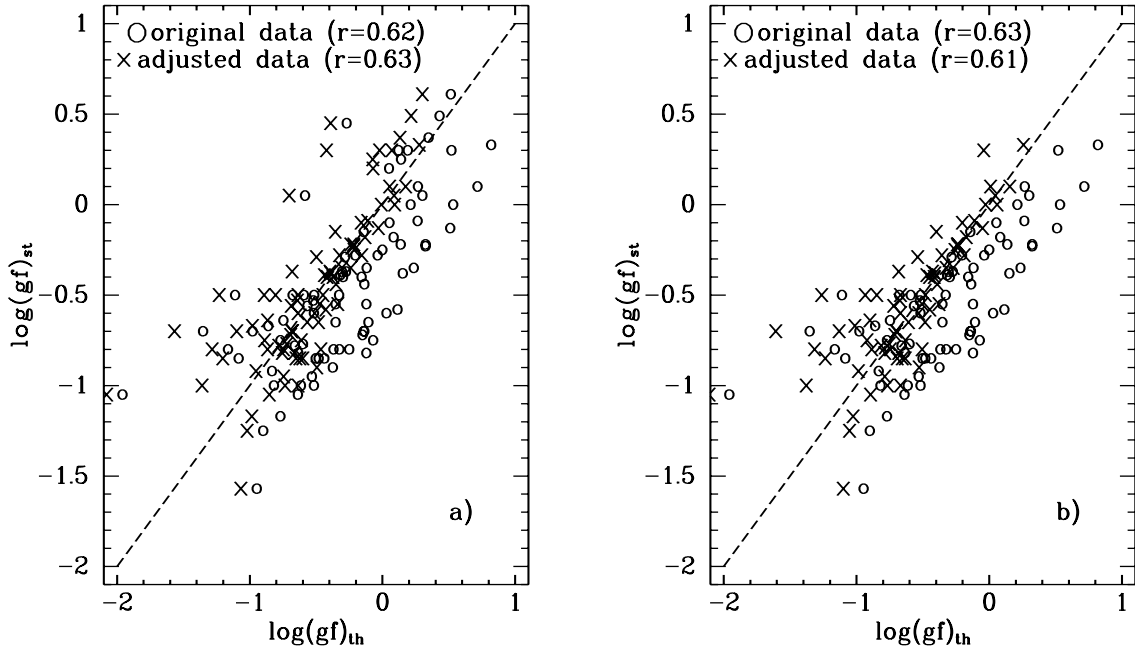
Fig. 1. Logarithm of stellar gf values as a function of the theoretical values. In both panels, the original data before any adjustment are indicated with circles and the data after adjusting the radial integrals are indicated with crosses. In panel **a)**, the adjustment for 84 Xe II lines is shown. In panel **b)**, nine lines have been eliminated (see text).

Table 1. continued.

λ (Å)	Conf.	$\log(gf_{st})$	$\log(gf_{th})$	$\log(gf_{th,ad1})$	$\log(gf_{th,ad2})$
5667.540	5d6p	−0.53	−0.5210	−0.6413	−0.6737
5699.610	5d6p	−0.85	0.1811		
5719.587	5d6p	−0.80	0.2181		
5726.880	5d6p	−0.28	−0.0370	−0.1570	−0.1894
5750.990	6s6p	−0.40	−0.1580	−0.3722	−0.4142
5758.665	5d6p	−0.35	−0.1190	−0.2391	−0.2715
5776.390	5d6p	−0.70	−0.9770	−1.0987	−1.1311
5893.290	5d6p	−0.90	−0.3750	−0.4946	−0.5270
5905.115	5d6p	−0.75	−0.7700	−0.8894	−0.9218
5945.530	5d6p	−0.67	−0.8590	−0.9800	−1.0124
5971.135	6s6p	−0.50	−0.5920	−0.8059	−0.8479
5976.460	6s6p	−0.29	−0.2830	−0.4973	−0.5393
6036.170	5d6p	−0.56	−0.5670	−0.6869	−0.7193
6051.120	5d6p	−0.28	−0.2050	−0.3247	−0.3571
6097.570	5d6p	−0.39	−0.3180	−0.4377	−0.4701
6101.370	5d6p	−0.50	−0.5160	−0.6356	−0.6680
6270.810	6s6p	−0.18	0.0810	−0.1314	−0.1734
6343.950	5d6p	−0.64	−0.7470	−0.8670	−0.8994
6375.280	5d6p	−1.00	−0.6150	−0.7343	−0.7667
6512.790	5d6p	−1.00	−0.5170	−0.6370	−0.6694
6528.650	5d6p	−0.40	−0.2970	−0.4166	−0.4490
6594.970	5d6p	0.00	0.2130	0.0923	0.0599
6597.230	5d6p	−0.60	−0.5170	−0.6370	−0.6694
6620.020	5d6p	−0.85	−1.0840	−1.2039	−1.2363
6694.285	5d6p	−0.92	−0.8330	−0.9526	−0.9850
6788.710	6s6p	−0.50	−0.6770	−0.8919	−0.9339
6790.370	6s6p	−0.70	−1.3530	−1.5668	−1.6088
6990.835	5d6p	0.30	0.1890	0.0705	
7082.150	5d6p	0.05	−0.5830	−0.7032	
7164.850	5d6p	0.20	0.0480	−0.0707	
7284.340	5d6p	−0.50	−1.1100	−1.2300	−1.2624
7339.300	5d6p	0.45	−0.2700	−0.3899	
7787.040	5d6p	−0.50	−0.3280	−0.4478	−0.4802

3.3.2. Individual behavior

We have taken 32 lines from the set of lines referred by Yuce et al. (2011) as without blend or noise; these are clearly isolated lines in the HR 6000 stellar spectrum (Castelli 2011). Wavelength, $\log(gf_{st})$, $\log(gf_{th})$, as well as $|gf_{st}-gf_{th}| * 100/gf_{st}$, are shown in Table 2 for these 32 lines. In Fig. 3 the logarithm of stellar gf values as a function of the theoretical value is shown for these 32 lines. It is clear that the theoretical and stellar values keep a reasonable ratio for these lines ($r = 0.87$). We must not forget that inaccuracies in the values of gf directly translate into inaccuracies in the calculation of stellar abundances.

4. Conclusions

The correlation between gf_{th}/gf_{st} and λ, made evident in Fig. 2, can be explained. On the one hand, the weaker a line, the more uncertain its astrophysical gf value. Since the gf values have a tendency to decrease as wavelength increases, the gf values of red lines are, in general, less accurate. On the other hand, the larger the wavelength, the larger the noise and the number of telluric lines in the spectra. This also lowers the accuracy of the results, as pointed out by Yuce et al. (2011). In general, our theoretical results (Table 1, Col. 4) are nearest other authors' theoretical or experimental results than they are to Yuce's results. For that reason, we are able to say that our theoretical gf values are more realistic that those by Yuce el al. (2011). But, when we consider unblended, relatively noise-free, and isolated lines, our theoretical gf values and Yuce's stellar values differ less from each other, as we see in Fig. 3.

Note the systematic shift due to plasma effects (Griem 1964) observed in the wavelength of the lines associated with the 6d and 7s Xe II energy levels from different spectral sources. Several works have been published on this topic by diverse authors, some as old as that by Di Rocco et al. (1986). Yuce et al. (2011) mention a discrepancy between their wavelengths measured from stellar spectra and those published by NIST, and they
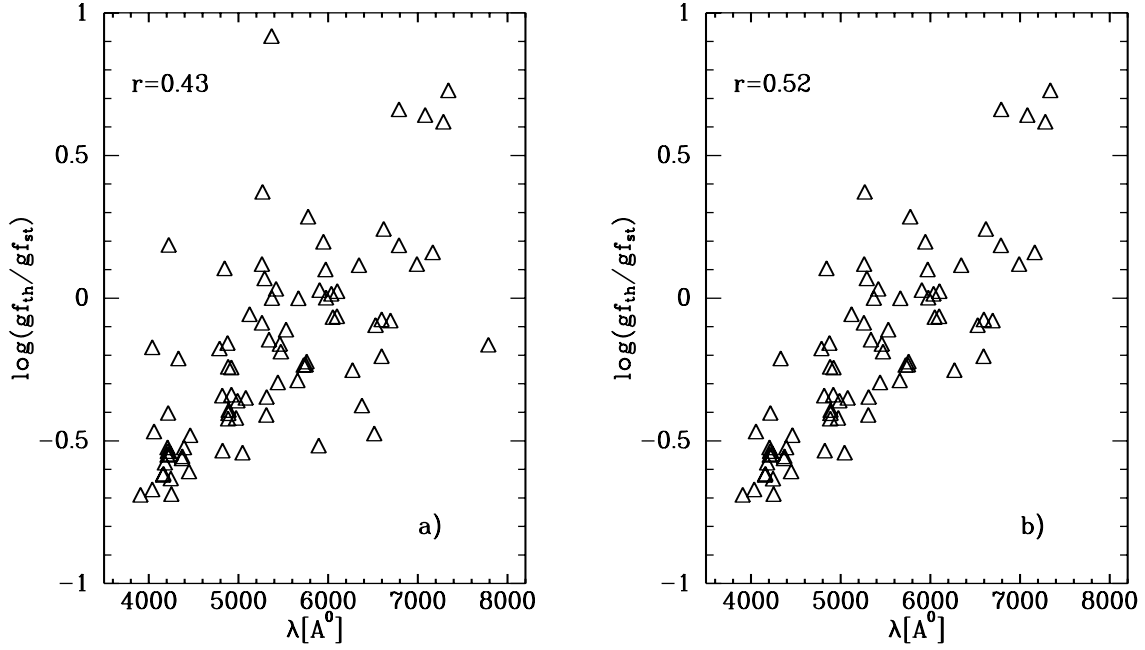
Fig. 2. gf_{th}/gf_{st} as a function of λ. In panel **a)** 84 lines are included. In panel **b)** seven lines have been removed (see text).

Table 2. Stellar and theoretical gf values for lines referred by Yuce et al. (2011) as without blend or noise in the HR 6000 stellar spectrum (Castelli 2011).

λ (Å)	Conf.	$\log(gf_{st})$	$\log(gf_{th})$	$|gf_{st} - gf_{th}|/gf_{st}$
4208.391	5d6p	–0.38	0.15	70.49
4222.900	6p6d	0.64	0.12	231.13
4238.135	6p6d	–0.23	0.32	71.82
4330.390	6p6d	0.30	0.52	39.74
4393.090	6p6d	0.00	0.53	70.49
4448.025	6p6d	0.15	0.72	73.08
4817.980	5d6p	–1.25	–0.90	55.33
4883.530	6s6p	–0.25	–0.00	43.77
4890.085	6s6p	–1.17	–0.77	60.19
4919.660	5d6p	–0.85	–0.50	55.33
4921.480	6s6p	0.05	0.30	43.77
4972.700	6s6p	–0.55	–0.12	62.85
5080.510	6p7s	–0.22	0.14	56.35
5261.950	6s6p	0.25	0.14	28.82
5292.220	6s6p	0.49	0.43	14.82
5313.760	6p7s	–0.09	0.27	56.35
5339.355	6s6p	–0.10	0.05	29.21
5419.155	6s6p	0.37	0.35	4.71
5438.960	6s6p	–0.44	–0.14	49.88
5460.365	5d6p	–0.77	–0.60	32.39
5472.600	5d6p	–0.55	–0.35	36.90
5531.050	5d6p	–0.78	–0.66	24.14
5667.540	5d6p	–0.53	–0.52	2.28
5905.115	5d6p	–0.75	–0.77	4.71
5976.460	6s6p	–0.29	–0.28	2.28
6036.170	5d6p	–0.56	–0.57	2.33
6051.120	5d6p	–0.28	–0.20	16.82
6097.570	5d6p	–0.39	–0.32	14.89
6343.950	5d6p	–0.64	–0.75	28.82
6512.790	5d6p	–1.00	–0.52	66.89
6694.285	5d6p	–0.92	–0.83	18.72
6990.835	5d6p	0.30	0.19	28.82

interpret the origin of this discrepancy as mostly due to incorrect energy levels. We establish now that, indeed, energy levels
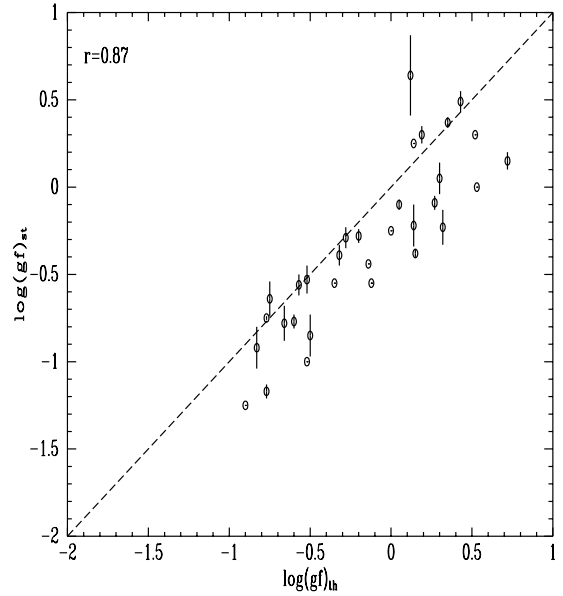

Fig. 3. Logarithm of stellar gf values as a function of the theoretical values for 32 isolated lines (see text). Error bars as given by Yuce et al. (2011) are indicated.

should undergo a shift in laboratory experiments. Therefore, it is clear that these lines are Xe II lines, but shifted by plasma effects, as explained above. In fact, modeling a perturbing potential by an expression of the form $V_k(r) = \sum_k C_k r^{-k}$, we can infer that the energy levels and, therefore, the atomic lines are shifted when the atom is inmersed in a plasma instead of being isolated. The case $k = 4$ is of paramount importance in taking collisions with electrons into account. In the semiclassical approximation (Griem 1964), both shifts and broadenings are proportional to $N_e T_e^{-1/2}$, where N_e and T_e are the electron density and electron temperature, respectively. In any case, stellar wavelengths could be considered the standard wavelengths whenever the densities in stellar atmospheres are smaller than 1×10^{16} part. cm^{-3}.

References

Boyce, J. C. 1936 , Phys. Rev., 49, 730
Castelli, F. 2011, http://wwwuser.oats.inaf.it/castelli/stars.html
Cowan, R. D. 1981, The Theory of Atomic Structure and Spectra (Berkeley, Los Angeles, London: University of California Press)
Di Rocco, H. O., Bertuccelli, G., Reyna Almandos, J. G., & Gallardo, M. 1986, J. Quant. Spectr. Rad. Transf., 35, 443
Di Rocco, H. O., Iriarte, D. I., & Pomarico, J. A. 2000, EPJD, 10, 19
Froese Fischer, C., Brage, T., & Jönsson, P. 1997, Computational Atomic Structure (Bristol and Philadelphia: IOP Publishing)
Gallardo, M., Raineri, M., & Almandos, J. G. Reyna 1993, Spectr. Lett., 26, 1241
Grant, I. P. 2007, Relativistic Quantum Theory of Atoms and Molecules (New York: Springer)
Griem, H. R. 1964, Plasma Spectroscopy (Berkeley, Los Angeles, London: University of California Press)
Griem, H. R. 1997, Principles of Plasma Spectroscopy (Cambridge: Cambridge University Press)
Gu, M. F. 2008, Can. J. Phys., 86, 675
Hansen, J. E., & Persson, W. 1987, Phys. Scr., 36, 602
Humphreys, C. J. 1939, J. Res. Natl. Bur. Stand. (US), 22, 19
Humphreys, C. J., de Bruin, T. L., & Meggers, W. F. 1931, J. Res. Natl. Bur. Stand. (US), 6, 287
Kramida, A., & Fuhr, J. R. 2015, http://physics.nist.gov/cgi-bin/ASBib1/TransProbBib.cgi, last updated March 2015, National Institute of Standards and Technology, Physical Measurement Laboratory, Quantum Measurement Division
Peláez, R. J., Djurovic, S., Cirisan, N., et al. 2009a, J. Phys. B: At. Mol. Opt. Phys., 42, 12, 7
Peláez, R. J., Cirisan, N., Djurovic, S., et al. 2009b, A&A, 507, 1697
Persson, W., Wahlström, C.-G., Bertuccelli, G., et al. 1988, Phys. Scr., 38, 347
Sahal-Bréchot, S., Dimitrijevic, M. S., & Ben Nessib, N. 2014, Atoms 2, 225
Saloman, E. B. 2004, J. Phys. Chem. Ref. Data, 33, 765
Sobelman, I.I., Vainshtein, L. A., & Yukov, E. A. 1995, Excitation of atoms and broadening of spectral lines (Springer)
Yüce, K., Castelli, F., & Hubrig, S. 2011, A&A, 528, A37